

AD-A172 997

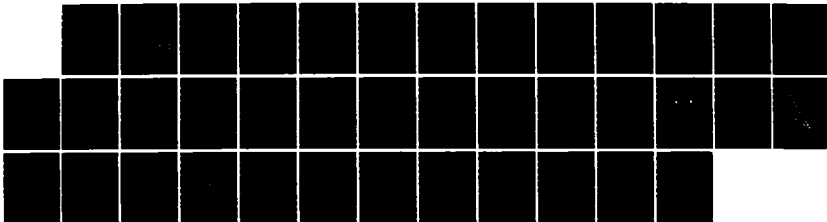
BLOW-OFF PRESSURES FOR ADHERING LAYERS(U) AKRON UNIV OH  
INST OF POLYMER SCIENCE A N GENT ET AL. NOV 86 TR-7  
N00014-85-K-0222

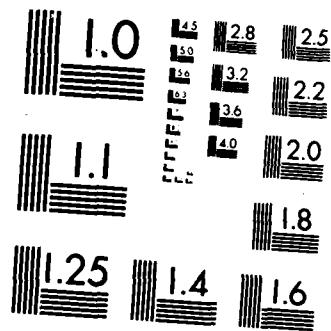
1/1

UNCLASSIFIED

F/G 11/1

NL





MICROCOPY RESOLUTION TEST CHART  
NATIONAL BUREAU OF STANDARDS-1963-A

12

AD-A172 997

OFFICE OF NAVAL RESEARCH

Contract N00014-85-K-0222

Project NR 092-555

Technical Report No. 7

BLOW-OFF PRESSURES FOR ADHERING LAYERS

by

A. N. Gent and L. H. Lewandowski

Institute of Polymer Science  
The University of Akron  
Akron, Ohio 44325

DTIC  
ELECTE  
OCT 9 1986  
S B

DTIC FILE COPY

November, 1986

Reproduction in whole or in part is permitted for any purpose  
of the United States Government.

Approved for Public Release; Distribution Unrestricted

86 10 8 145

REPORT DOCUMENTATION PAGE		READ INSTRUCTIONS BEFORE COMPLETING FORM
1. REPORT NUMBER Technical Report No. 7	2. GOVT ACCESSION NO. AD-A172 997	3. RECIPIENT'S CATALOG NUMBER
4. TITLE (and Subtitle) Blow-Off Pressures for Adhering Layers	5. TYPE OF REPORT & PERIOD COVERED Technical Report	
	6. PERFORMING ORG. REPORT NUMBER	
7. AUTHOR(s) A. N. Gent and L. H. Lewandowski	8. CONTRACT OR GRANT NUMBER(s) N00014-85-K-0222	
9. PERFORMING ORGANIZATION NAME AND ADDRESS Institute of Polymer Science The University of Akron Akron, Ohio 44325	10. PROGRAM ELEMENT, PROJECT, TASK AREA & WORK UNIT NUMBERS NR 092-555	
11. CONTROLLING OFFICE NAME AND ADDRESS Office of Naval Research Power Program Arlington, VA 22217	12. REPORT DATE November, 1986	
	13. NUMBER OF PAGES 35	
14. MONITORING AGENCY NAME & ADDRESS (if different from Controlling Office)	15. SECURITY CLASS. (of this report) Unclassified	
	15a. DECLASSIFICATION/DOWNGRADING SCHEDULE	
16. DISTRIBUTION STATEMENT (of this Report) According to attached distribution list. Approved for public release; distribution unrestricted.		
17. DISTRIBUTION STATEMENT (of the abstract entered in Block 20, if different from Report)		
18. SUPPLEMENTARY NOTES Submitted for publication in: Journal of Applied Polymer Science		
19. KEY WORDS (Continue on reverse side if necessary and identify by block number) Adhesion, Blister Test, Bonding, Debonding, Detachment, Pressure Test, Tapes.		
20. ABSTRACT (Continue on reverse side if necessary and identify by block number) An analysis is given of the critical internal pressure $P$ at which a circular debond ("blister") will grow in size, in terms of the tensile modulus $E$ and thickness $t$ of an adhering layer, and the strength $G_a$ of its adhesion to a rigid substrate. Measurements of blow-off pressure are reported for adhering layers of pressure-sensitive tapes having widely-different effective modulus and thickness, and with blisters having a range of diameters. Satisfactory agreement is obtained with the theoretical		

predictions, suggesting that the theory is basically correct in assuming that relatively thin layers behave like elastic membranes. Attention is drawn to the unusual form of the dependence of the debonding pressure  $P$  upon the resistance  $E_t$  of the layer to stretching and upon the detachment energy  $G_a$ :  $P^4 \propto E_t G_a^3$ . Even though the adhering layer is assumed to be linearly-elastic, the markedly non-linear (cubic) relation between pressure  $P$  and volume  $V$  of the blister, or maximum height  $y$ , leads to this unusual result. The detachment energy is given by a particularly simple function of the pressure  $P$  and maximum deflection  $y$  of the blister:  $G_a = 0.65 Py$ , independent of the stiffness of the adhering layer and diameter of the blister.

Accession For	
NTIS	<input checked="" type="checkbox"/>
DTIC	<input type="checkbox"/>
Unannounced	<input type="checkbox"/>
Just	<input type="checkbox"/>
By	
Distrib	
Avail	
Dist	
A-1	

## 1. Introduction

A pressurized blister test is a possible way of measuring the strength of adhesion between a deformable adhering layer and a rigid substrate. It was recommended by Dannenberg (1) and adopted by Williams and colleagues (2, 3) and Andrews and Stevenson (4) to study adhesion in selected systems. Interpretation of the measurements is not a simple matter, however. Three experimental situations can be distinguished: (i) the blister diameter is much smaller than the thickness of the adhering layer, (ii) the blister diameter is comparable to the thickness of the adhering layer, and, (iii) the blister diameter is much larger than the thickness of the adhering layer.

Correspondingly, there are three different principal modes of deformation in the pressurized layer: (i) mainly in highly-stressed regions around the edge of the blister diameter, (ii) mainly in bending deformation of the adhesive layer, regarded as a flexible circular plate with a built-in edge constraint, and, (iii) mainly in tensile deformation of the adhesive layer, regarded as an elastic membrane.

In each case, by analysing the changes in stored elastic energy that take place as the blister grows and equating them to the energy required to separate the adhering layer from the substrate, values can be obtained for the critical pressure  $\underline{P}$  for growth of the blister. In the first case, the result is (2, 5)

$$(i) \quad P^2 = 2\pi E G_a / 3a \quad (1)$$

and in the second case (6),

$$(ii) \quad P^2 = 128 E G_a t^3 / 9a^4, \quad (2)$$

where  $\underline{E}$  denotes the tensile (Young's) modulus of the adhering layer,  $\underline{G}_a$  is the energy required for detachment per unit of interfacial area (a measure of

the strength of adhesion),  $a$  is the radius of the blister, and  $t$  is the thickness of the deformable layer. For the third case, when the blister radius is relatively large compared to the layer thickness, the result, given in the Appendix, is

$$P^4 = 17.4 EG_a^3 t/a^4. \quad (3)$$

It is surprisingly different in form to the preceding results. The critical pressure is less strongly dependent upon the tensile modulus and thickness of the adhering layer and more strongly dependent upon the strength of adhesion than before. These marked differences arise from the different elastic response of a membrane to internal pressure in comparison with a plate. Deflections of a plate are directly proportional to the applied pressure, whereas deflections of a membrane are proportional to the one-third power of the inflating pressure (7) (it being assumed in both cases that the deflections are small).

In view of the serious consequences of delamination due to pressure in coatings and sealants, it is important to examine the validity of equation 3 thoroughly. Also, as suggested by Hinckley (8), a pressurized blister test may prove to be a good method of measuring interfacial adhesion. A detailed experimental study has therefore been carried out of the elastic deformation and critical debonding pressures for elastic layers adhering to rigid substrates. The layers consisted of commercial adhesive tapes, chosen for their widely-different elastic modulus. They were applied in multiple layers, so that the tensile stiffness of the composite layer could be changed substantially without any change in the strength of adhesion. They were also applied to two different substrates; Plexiglas and Teflon; so that the strength of adhesion could be changed (at least, in principle) without any

change in the elastic properties of the tape. The experimental procedures and results are described below.

## 2. Experimental

Two commercial pressure-sensitive tapes were employed: A, an electrical tape with an acrylic adhesive layer and a soft vinyl backing, having a thickness of about 0.18 mm (Tape No. 35, 3M Company); B, a packing tape with a biaxially-oriented polypropylene backing, having a thickness of about 0.09 mm (Tape No. 375, 3M Company). They were chosen because they had similar strengths of adhesion to Plexiglas and Teflon but quite different tensile properties. As shown in Figure 1, tape A gave an approximately linear relation between tensile stress and extension over the range 0 to 20 per cent extension whereas tape B underwent plastic yielding at a tensile strain of about 2-3 per cent. Below this strain, however, the stress-strain relation was substantially linear and a value for the tensile stiffness  $\underline{Et}$  per unit width could be estimated. Experimentally-determined values at a rate of extension of  $1 \times 10^{-6} \text{ s}^{-1}$ , corresponding to the approximate rate of extension in the blow-off experiments described later, were  $900 \pm 150 \text{ N/M}$  for tape A and  $105 \pm 15 \text{ kN/M}$  for tape B. Using the measured thicknesses  $\underline{t}$ , these results correspond to effective values of tensile modulus  $\underline{E}$  of 5.0 MPa and 1.2 GPa, respectively.

The tapes showed some anisotropy in elastic behavior. Tape A was stiffer in the machine direction in comparison with the transverse direction by about 30 per cent, whereas tape B was stiffer in the transverse direction by about 30 per cent. Values for  $\underline{Et}$  given above are averages for the two directions.

A layer of each tape was adhered to a flat plate of Plexiglas containing a central circular depression, about 1 mm deep and having a diameter of 25,



50 or 75 mm. The tape stretched over the circular depression without adhering to its base, so that an initial debond of well-defined shape and size was obtained. The depression was filled with a silicone vacuum grease also, to prevent any adhesion.

For studies of the elastic behavior, a rigid circular clamp was employed to secure the tape against the Plexiglas plate at the edge of the circular depression, Figure 2a. The effective diameter of the elastic membrane was then the same as that of the circular depression. In blow-off experiments this clamping ring was omitted, Figure 2b. Then, at a critical inflation pressure, further debonding took place at the edges of the circular depression. Measurements were made of the diameter, volume and height of the debonded region ("blister") and of the corresponding pressure required to make it grow, as the mean diameter of the blister increased from its initial value to a maximum value of about 75 mm.

The inflation pressure was measured using a mercury manometer for tape A, and a calibrated Bourdon gauge for tape B when the values were considerably higher, approaching 1 atmos. The volume V of the blister was measured by metering the quantity of water injected into the debond through a small hole in the center of the circular depression, Figure 2. The deflection y of the center of the blister away from the undeformed plane was measured with a cathetometer. All measurements were carried out at ambient temperature, about 25°C, and at a rate of inflation of the blister of about 0.3 ml/min corresponding to a rate of growth of the blister radius of the order of 1 mm/min.

Peeling measurements were carried out at a peel angle of  $90^\circ$  and at the same rate, 1 mm/min, in order to determine the detachment energy  $G_a$  directly for each tape and substrate combination:

$$G_a = F/w \quad (4)$$

where  $F$  is the peel force and  $w$  is the width of the tape.

### 3. Experimental Results and Discussion

#### Elastic behavior

When the radius of the blister was held constant by a clamping ring, Figure 2a, its volume  $V$  was found to be proportional to the deflection  $y$  of the center, as shown in Figure 3. Thus,

$$V = C_1 \pi a^2 y \quad (5)$$

where  $\pi a^2$  is the area debonded and  $C_1$  is an experimentally-determined constant, 0.52, in good agreement with Hencky's theoretical result (7), given in the Appendix,  $C_1 = 0.519$ .

Experimental relations between inflation pressure  $P$  and maximum deflection  $y$  are given in Figure 4 for layers of tape  $A$ . Several layers were plied together to give a composite membrane with a tensile stiffness that was a simple multiple of the value for a single layer. The layers were secured with a clamping ring, as shown in Figure 2a, to hold the blister radius  $a$  constant during inflation. In each case the pressure  $P$  was found to be proportional to  $y^3$ , as shown in Figure 4, in good agreement with the theory of elastic membranes (see Appendix, equation A.2) and also proportional to the number  $N$  of layers plied together.

$$P = C_2' E t y^3 / a^4 \quad (6)$$

From the slopes of the experimental relations, values of the tensile stiffness coefficient  $E_t$  were calculated by means of equation A.2, using Hencky's value for the coefficient  $C_2'$  of 4.75 (7). The results were closely similar for blister radii of 12.5 and 25 mm:  $E_t = 1.01$  kN/m; and in good agreement with the value measured directly by tensile experiments on tape A,  $E_t = 0.90$  kN/m. Similar measurements with the stiffer tape B gave less satisfactory agreement, however. Values of  $E_t$  of  $45 \pm 5$  kN/m were deduced from inflation measurements using equation 6, whereas the directly measured value was considerably larger, 105 kN/m. This discrepancy may arise from difficulties in clamping the stiff tape B firmly at the edge of the blister during inflation experiments.

#### Debonding conditions

Typical experimental relations for tape B between inflating pressure  $P$ , maximum deflection  $y$ , and radius  $a$ , are shown in Figures 5 and 6. Initially, the membrane inflated into a blister with increasing height  $y$  with increasing pressure, but with the original radius  $a_0$  of the circular debond. Then, at a critical pressure  $P_c$ , further debonding started and the pressure fell continuously as the blister grew in radius.

Actually, a small amount of debonding took place with increasing pressure, so that the radius of the initial blister grew by about 1 mm before the critical pressure was reached. After this, however, further growth of the blister took place with steadily-decreasing pressures, as the theory predicts (see Appendix). The anomalous behavior observed at the start is attributed to weak adhesion at the edges of the original blister, possibly due to entrapment of silicone grease there.

One of the theoretical predictions is that the product  $\underline{P}\underline{y}$  is a constant, directly related to the characteristic fracture energy  $\underline{G}_a$  for the bond, equation A.9. The broken curve in Figure 5 is of this form, with the constant chosen to give best agreement with the experimental measurements. As can be seen, the experimental results agree reasonably well with the predicted dependence of  $\underline{P}$  on the blister height  $\underline{y}$ . Similarly, the broken curve in Figure 6 is of the theoretical form, equation A.10;  $\underline{P}_a = \text{constant}$ ; and again the constant has been chosen to give best agreement with the experimental measurements. And again the agreement is relatively good.

On the other hand, less satisfactory agreement was obtained with the softer tape A, as shown in Figures 7 and 8. During debonding the pressure  $\underline{P}$  fell more rapidly as the blister height  $\underline{y}$  and the radius  $\underline{a}$  increased than an inverse proportionality would predict. This is attributed to a dependence of the fracture energy  $\underline{G}_a$  upon the rate of detachment. During the blow-off experiments the effective rate of peeling changed, being initially more rapid and later slowing down, because of the way in which the experiments were conducted. The blister was inflated at a constant rate of volume increase, of about 0.3 ml/min, and not at a constant rate of increase of radius. Peel experiments revealed that the fracture energy for tape A depended strongly upon the rate of peel, increasing by about 50 per cent for a ten-fold increase in rate. Thus, the products  $\underline{P}\underline{y}$  and  $\underline{P}_a$  would be expected to have larger values initially, and smaller values later, as was observed in the experiments, Figures 7 and 8, because of a continuous decrease in the effective peel rate.

### Fracture energies

Average values of the products  $\underline{P}_y$  and  $\underline{P}_a$  were obtained from experimental relations like those shown in Figures 5-8. They are listed in Table 1, together with values of the fracture energy  $\underline{G}_a$  calculated from them by means of equations A.9 and A.10, respectively, using experimentally-determined values of the tensile stiffness coefficients  $\underline{E}_t$  in the latter case.

In all cases, values deduced for  $\underline{G}_a$  from  $\underline{P}_a$  and  $\underline{P}_y$  are seen to be in excellent agreement. They range from about 15 J/m<sup>2</sup> up to about 150 J/m<sup>2</sup>, within the general range expected for pressure-sensitive adhesives, and they are distinctly smaller for a Teflon substrate, as would be expected. However, larger values were obtained by peeling strips of the same tapes away from the same substrates at 90°, given in the final column of Table 1. Similar discrepancies were noted before in comparing values of  $\underline{G}_a$  obtained from pull-off experiments at shallow angles with those obtained from 90° peel tests (9). It was suggested then that the severe bending experienced by tapes in peeling at 90° may lead to additional energy being expended in dissipative processes. Further experiments are necessary to decide whether this factor is indeed responsible for the differences in  $\underline{G}_a$  from the two types of detachment.

#### 4. Conclusions

The following conclusions are obtained:

- (i) Adhesive layers can be regarded as elastic membranes when a circular debond ("blister") at the interface is pressurized. As a result, the relation between inflation pressure and blister volume or blister height is approximately a cubic one until the blister starts to increase in radius by further debonding.
- (ii) When an energy balance is applied to determine the conditions for growth of the blister by further debonding, a particularly simple relation is found to hold between the fracture energy  $G_a$  and the corresponding values of debonding pressure  $P$  and blister height  $y$ :
$$G_a = 0.65 Py,$$
independent of the radius of the blister or of the stiffness of the adhering layer.
- (iii) Qualitatively similar conclusions were reached previously by Hinckley (8). The quantitative differences are discussed in the Appendix.
- (iv) Measurements on two pressure-sensitive tapes, adhering to two different substrates, have been compared with the theoretical predictions. Although agreement is generally satisfactory, values deduced for the fracture energy  $G_a$  are consistently smaller than those obtained by peeling strips of the same tapes away from the same substrates at an angle of  $90^\circ$ . A similar discrepancy was noted in an

earlier study of detachment at shallow angles (9). It is provisionally attributed to additional energy dissipation in the tape backing when it is bent sharply away from the substrate at  $90^\circ$ .

Acknowledgements

This work was supported by a research contract from the Office of Naval Research (N00014-85-K-0222) and by an educational grant from the Adhesive and Sealant Council. The authors also acknowledge helpful discussions with Professor D. R. Bowman of The University of Akron, Prof. R. Fosdick of the University of Minnesota, and Prof. S. Senturia of Massachusetts Institute of Technology, on the mechanics of pressurized membranes, and the supply of adhesive tapes by Dr. L. M. Clemens of 3M Company.



References

1. H. Dannenberg, J. Appl. Polym. Sci. 5, 125-134 (1961).
2. M. L. Williams, J. Appl. Polym. Sci. 13, 29-40 (1969).
3. S. J. Bennett, K. L. DeVries and M. L. Williams, Int. J. Fracture 10, 33-43 (1974).
4. E. H. Andrews and A. Stevenson, J. Mat. Sci. 13, 1680-1688 (1978).
5. V. I. Mossakovskii and M. T. Rybka, PMM 28, 1061 (1964); J. Appl. Math. Mech. 28, 1277 (1964).
6. M. L. Williams, Proc. 5th U. S. Natl. Congr. Appl. Mech., Minneapolis, June 1966, A.S.M.E., New York, 1966, p. 451.
7. H. Hencky, Zeitschr. f. Math. u. Phys. 63, 311-317 (1915).
8. J. A. Hinckley, J. Adhesion 16, 115-126 (1983).
9. A. N. Gent and S. Y. Kaang, J. Appl. Polym. Sci., in press.
10. W. Z. Chien, Sci. Rep. Natn. Tsing Hua Univ. A5, 71-94 (1948).
11. R. W. Dickey, Arch. Ration. Mech. Anal. 26, 219-236 (1967).
12. R. Kao and N. Perrone, Int. J. Solids Structures 7, 1601-1612 (1971).
13. A. Kelkar, W. Elber and I. S. Raju, Computers and Structures 21, 413-421 (1985).
14. R. M. Christensen and W. W. Feng, J. Rheol. 30(1), 157-165 (1986).

### Appendix

Theoretical relations for the deformation of a circular elastic membrane under a uniform pressure are reviewed below, and then employed to calculate the blow-off pressure for an adhesive layer containing a circular debond.

#### (i) Elastic deformation

Inflation of a thin circular elastic membrane, clamped at the periphery, has been analyzed by several authors. The results take the form:

$$V = C_1 \pi a^2 y \quad (\text{A.1})$$

and

$$y = C_2 (Pa^4/Et)^{1/3} \quad (\text{A.2})$$

where  $V$  is the volume of the "blister",  $y$  is the deflection of the center away from the membrane plane in the undeformed state,  $a$  and  $t$  are the radius and thickness of the membrane,  $E$  is Young's modulus for the membrane material,  $P$  is the inflating pressure and  $C_1$  and  $C_2$  are numerical coefficients whose values depend upon the value of Poisson's ratio  $\nu$ . Using series expansions, Hencky (7) obtained values of  $C_1 = 0.518$  and  $C_2 = 0.662$  for  $\nu = 0.3$ . Using his procedures, values of  $C_1 = 0.519$  and  $C_2 = 0.595$  are obtained when  $\nu = 0.5$ , i.e., for incompressible elastic layers, like rubber.

It should be noted, however, that other authors, using different starting points or purely numerical methods, have obtained slightly different values of  $C_2$  than Hencky for  $\nu = 0.3$ : 0.653, 0.654 (10-13) but the same value when  $\nu = 0.5$ :  $C_2 = 0.595$  (11). When the considerable approximation is made that the inflated membrane takes up the shape of a spherical cap, values of the coefficients are obtained that are at most only about 4 per cent smaller than Hencky's:  $C_1 = 0.5$  for  $\nu = 0.3$  or 0.5; and  $C_2 = 0.640$  or 0.572 for  $\nu = 0.3$  or 0.5, respectively (14).

Thus, there is a substantial level of agreement, although not complete, on the elastic deformation of an inflated membrane. In the analysis of debonding mechanics given below the deformation of the membrane is assumed to be that derived by Hencky.

(ii) Blow-off pressure.

An energy criterion for debonding is assumed to hold in which energy  $\Delta W$  supplied to the system as the circular debond increases in radius by a small amount  $\Delta a$  is equated to energy expended in the debonding process itself. Changes in elastic energy in the membrane must also be taken into account. Thus,

$$\Delta W = \Delta W_1 + \Delta W_2 \quad (\text{A.3})$$

where the input energy  $\Delta W = P\Delta V$ ,  $\Delta W_1$  denotes energy expended in detachment, given in terms of the characteristic energy  $G_a$  of detachment per unit area of bond by

$$\Delta W_1 = 2\pi a G_a \Delta a, \quad (\text{A.4})$$

and  $\Delta W_2$  denotes the change in energy stored elastically in the stretched membrane as the radius of the debond increases by an amount  $\Delta a$ .

Input energy  $\Delta W$  is given by

$$\Delta W \equiv P(\partial V/\partial a)_P \Delta a = (10 PV/3a)\Delta a \quad (\text{A.5})$$

from equations A.1 and A.2.

On integrating the cubic relation between pressure and volume for a blister of constant radius  $a$ , equations A.1 and A.2, the amount of energy stored in the inflated membrane is obtained as

$$W_2 = PV/4. \quad (\text{A.6})$$

Thus, as the radius of the blister increases by an amount  $\Delta a$  the energy term  $W_2$  changes by an amount:

$$\Delta W_2 = P(\partial V/\partial a)_P \Delta a/4 = \Delta W/4. \quad (\text{A.7})$$

On substituting from equations A.4, A.5 and A.7 in equation A.3, the detachment energy  $G_a$  is obtained as

$$G_a = 0.398 PV/a^2 \quad (\text{A.8})$$

or

$$G_a = 0.649 Py. \quad (\text{A.9})$$

The blow-off pressure is then obtained in terms of the blister radius  $a$  by means of equation A.2,

$$P^4 = 17.4 Et G_a^3/a^4. \quad (\text{A.10})$$

The main features of this analysis were recognized by Hinckley in 1983 (8): that the elastic behavior of an inflated blister follows membrane theory; that the relation between pressure  $P$  and deflection  $y$  will therefore be a cubic one; and

that an energy balance can be applied to determine the conditions for growth of the blister by further debonding. However, the treatment given here differs from that of Hinckley in two respects: the approximation of the shape of the blister by a spherical cap is not made; instead, the detailed analysis of Hencky is employed; and, more importantly, the energy balance given in equation A.3 is used in place of that proposed by Hinckley, which takes the form

$$\Delta W_1 = \Delta W_2 \quad (\text{A.11})$$

in the present notation, and is thought to be incorrect. As a result, Hinckley obtained the relation

$$G_a = 0.25 Py \quad (\text{A.12})$$

in place of equation A.9.

Table 1: Fracture energies  $G_a$  ( $J/m^2$ ) from blow-off and from peeling experiments.

Number N of layers	$\overline{Pa}$ (N/m)	$\overline{Py}$ (N/m)	$\overline{Ga}$ (calc. from Pa)	$\overline{Ga}$ (calc. from Py)	$\overline{Ga}$ (from peeling)
Tape <u>A</u> on Plexiglas substrate					
1	129 ± 11	38 ± 5	26 ± 3	24.5 ± 3	45.2 ± 3
2	155 ± 13	38 ± 3.5	26.5 ± 3	24.5 ± 2.5	
3	165 ± 27	36 ± 7	24.5 ± 5.5	23.5 ± 4.5	
5	175 ± 25	33 ± 6	23 ± 4.5	21.5 ± 3.5	
7	190 ± 15	32 ± 3.5	22.5 ± 2.5	20.8 ± 2.1	
10	195 ± 25	32 ± 5	21 ± 3.5	20.8 ± 3.4	
Tape <u>A</u> on Teflon substrate					
1	101 ± 7	22.3 ± 2.5	18.5 ± 2	14.5 ± 1.5	46.2 ± 1.5
Tape <u>B</u> on Plexiglas substrate					
1	1575 ± 65	237 ± 12	150 ± 8	154 ± 8	228 ± 12
Tape <u>B</u> on Teflon substrate					
1	375 ± 10	41.5 ± 1.5	22.2 ± 1	26.9 ± 1	95.5 ± 6

Figure Captions

1. Relations between tensile force per unit width  $\underline{F/w}$  and extension  $\underline{e}$  for tapes A and B.
2. (a) Measurement of elastic behavior of a pressurized membrane, radius  $\underline{a_0}$ .  
(b) Measurement of blow-off pressures and deflections.
3. Experimental relation between blister volume  $\underline{V}$  and height  $\underline{y}$  for clamped layers having a radius  $\underline{a_0}$  of 38 mm.  $\circ$ , two layers of tape B;  $\nabla$ , 5 layers of tape A.
4. Experimental relations between inflation pressure  $\underline{P}$  and blister height  $\underline{y}$  for clamped layers of tape A having a radius  $\underline{a_0}$  of 25 mm.  $\underline{N}$  denotes the number of layers plied together.
5. Experimental relation between inflation pressure  $\underline{P}$  and maximum height  $\underline{y}$  of the blister for one layer of tape B. The broken curves are of the theoretical forms:  $\underline{P} \propto \underline{y}^3$ , equation A.2, for inflation; and  $\underline{P} \propto 1/\underline{y}$ , equation A.9, for debonding.
6. Experimental relation between inflation pressure  $\underline{P}$  and blister radius  $\underline{a}$  for one layer of tape B. The broken curve is of the theoretical form, equation A.10,  $\underline{Pa} = \text{constant}$ .
7. Experimental relation between inflation pressure  $\underline{P}$  and maximum height  $\underline{y}$  of the blister for one layer of tape A with an initial debond radius  $\underline{a_0} = 12.5 \text{ mm}$ . The broken curve is of the theoretical form;  $\underline{Py} = \text{constant}$ , equation A.9.

8. Experimental relation between inflation pressure  $P$  and blister radius  $a$  for one layer of tape  $A$ . The broken curve is of the theoretical form;  $Pa = \text{constant}$ , equation A.10.



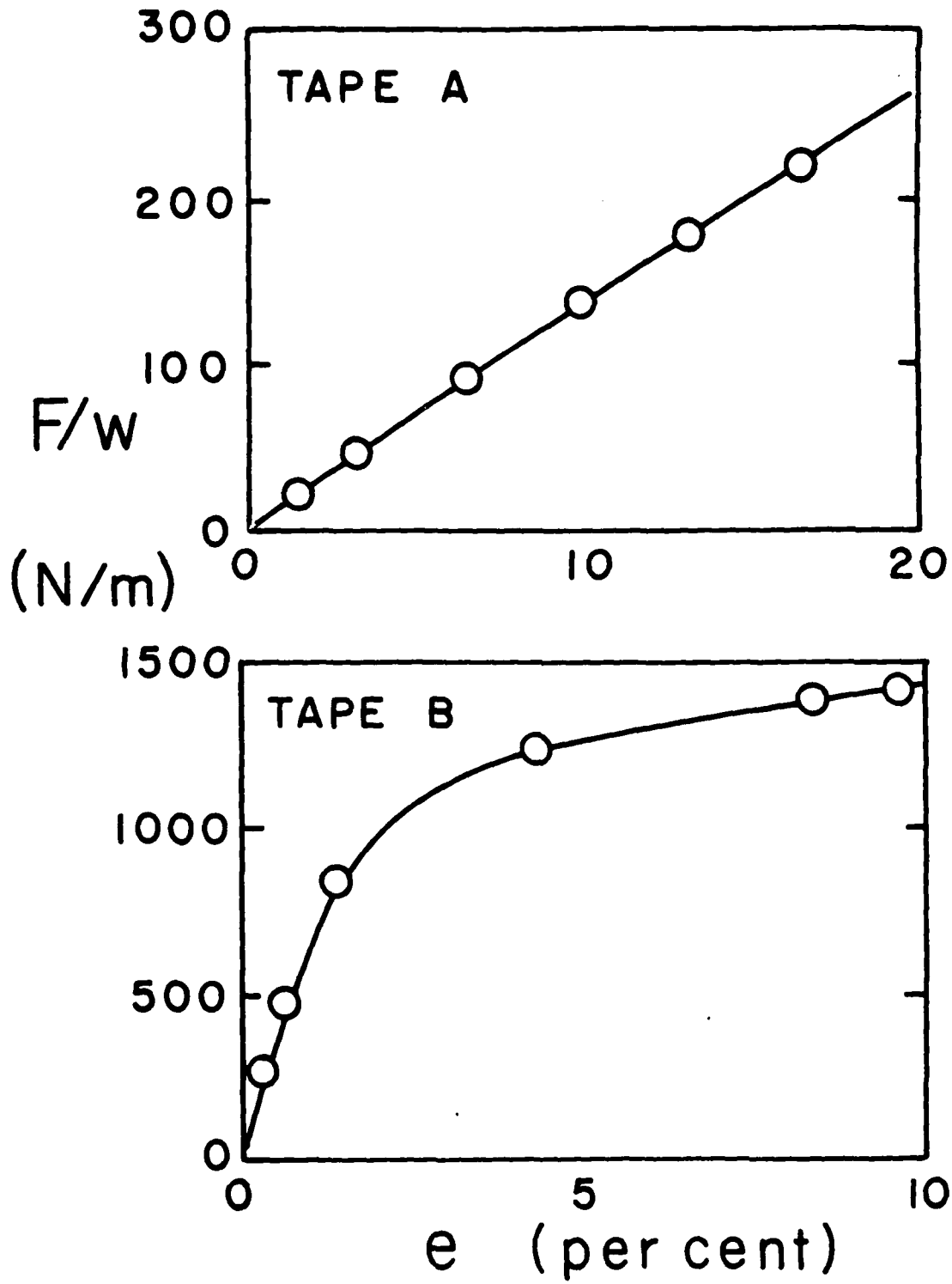


Figure 1

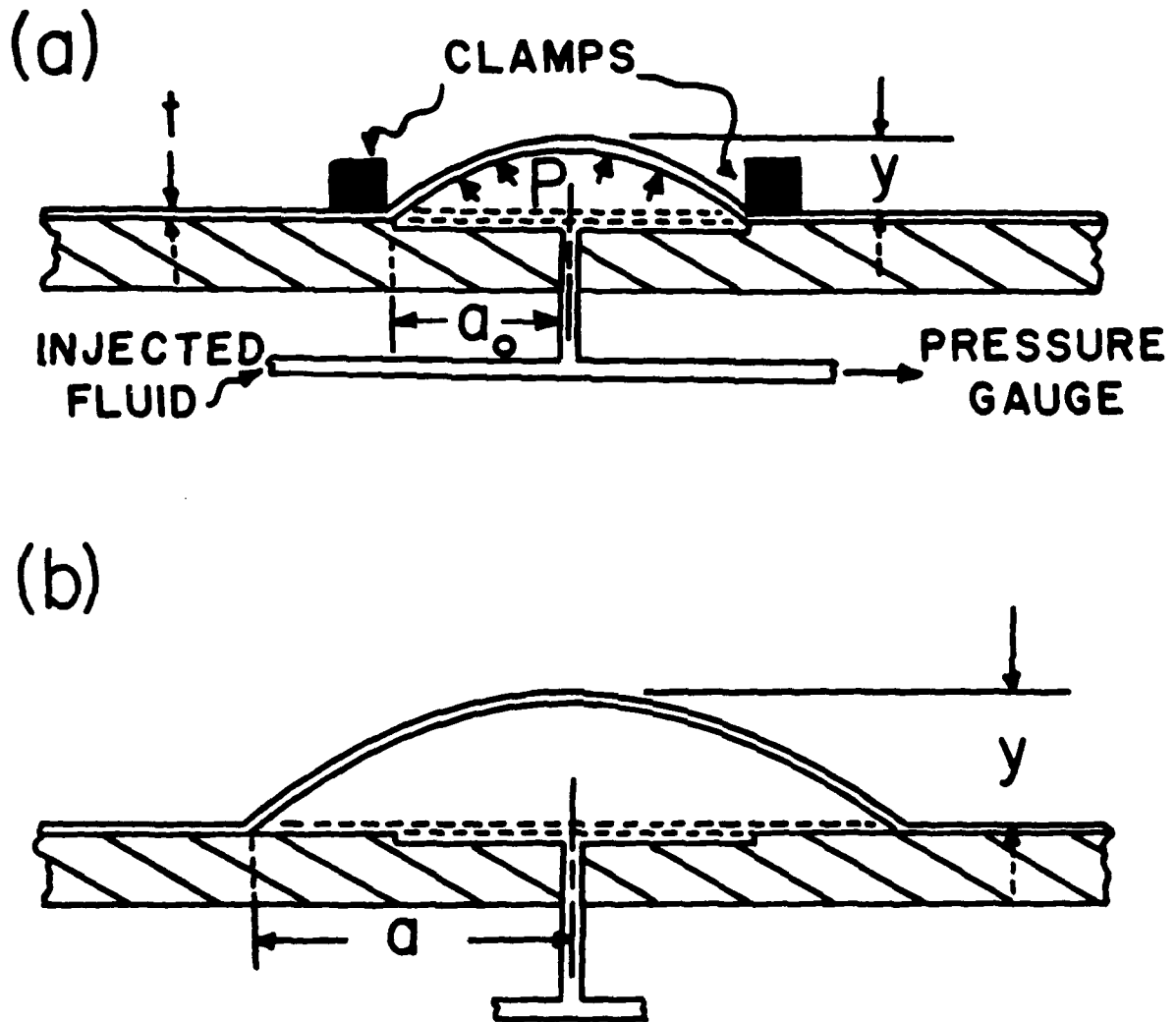


Figure 2

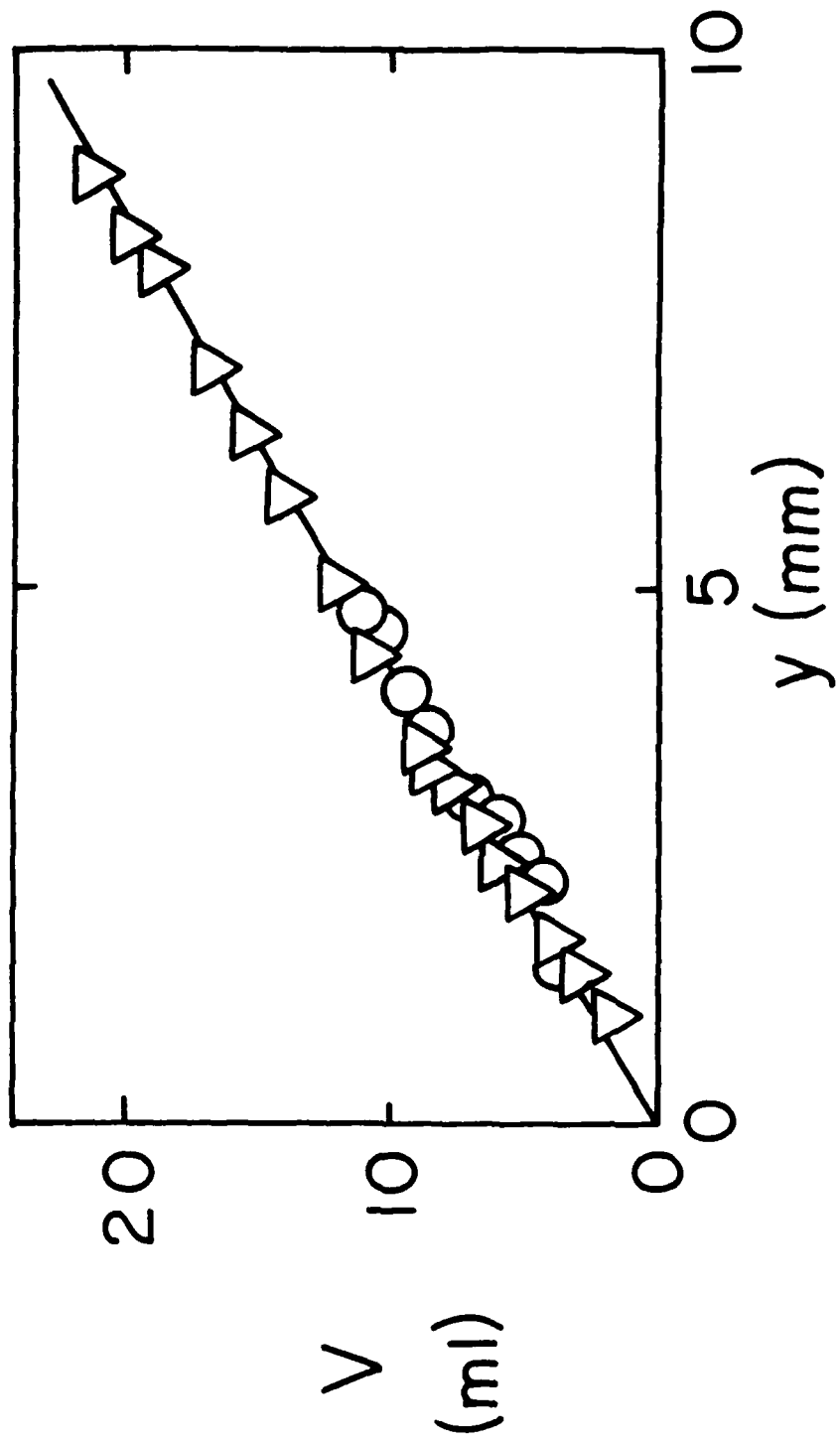


Figure 3

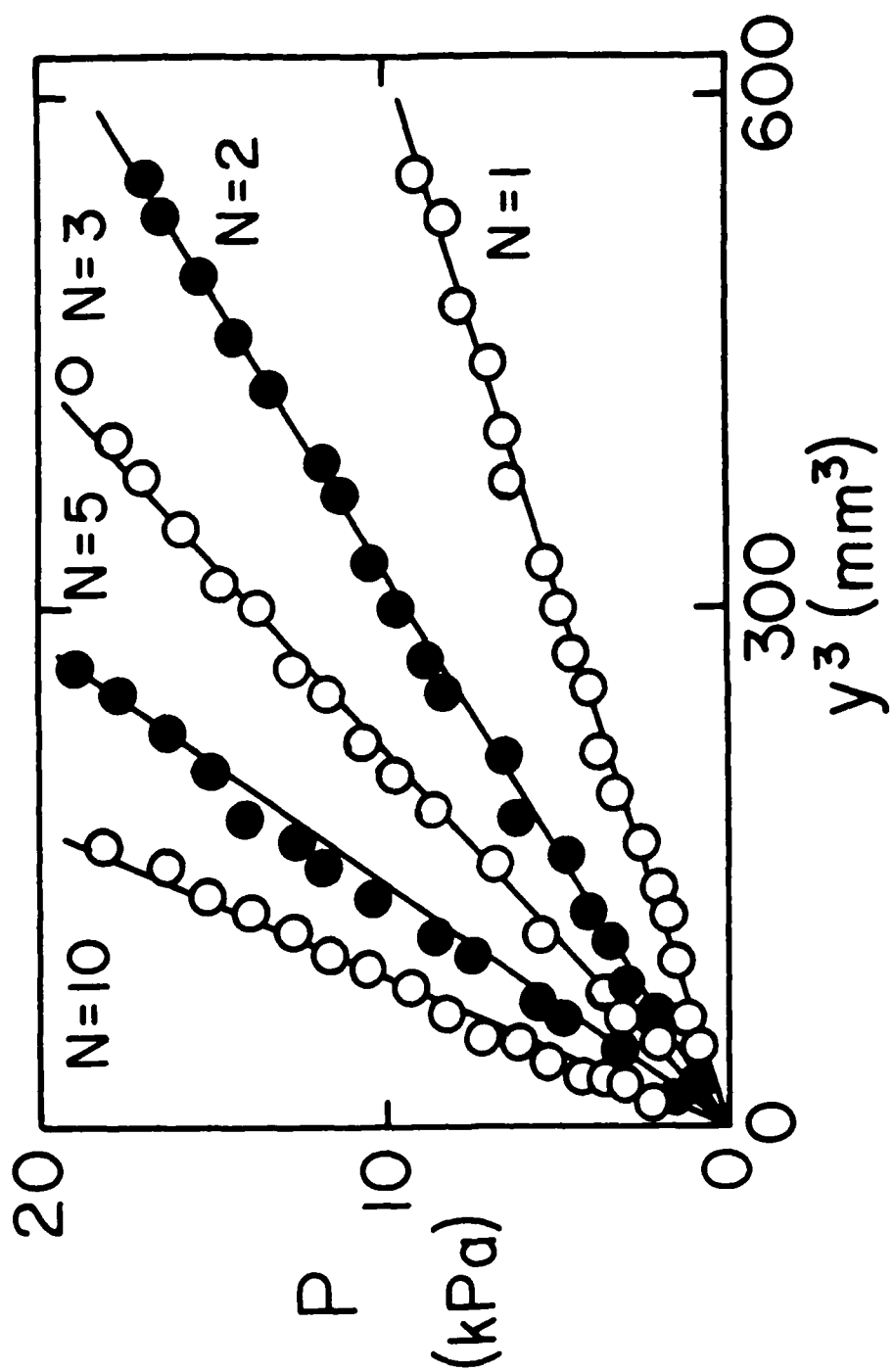


Figure 4

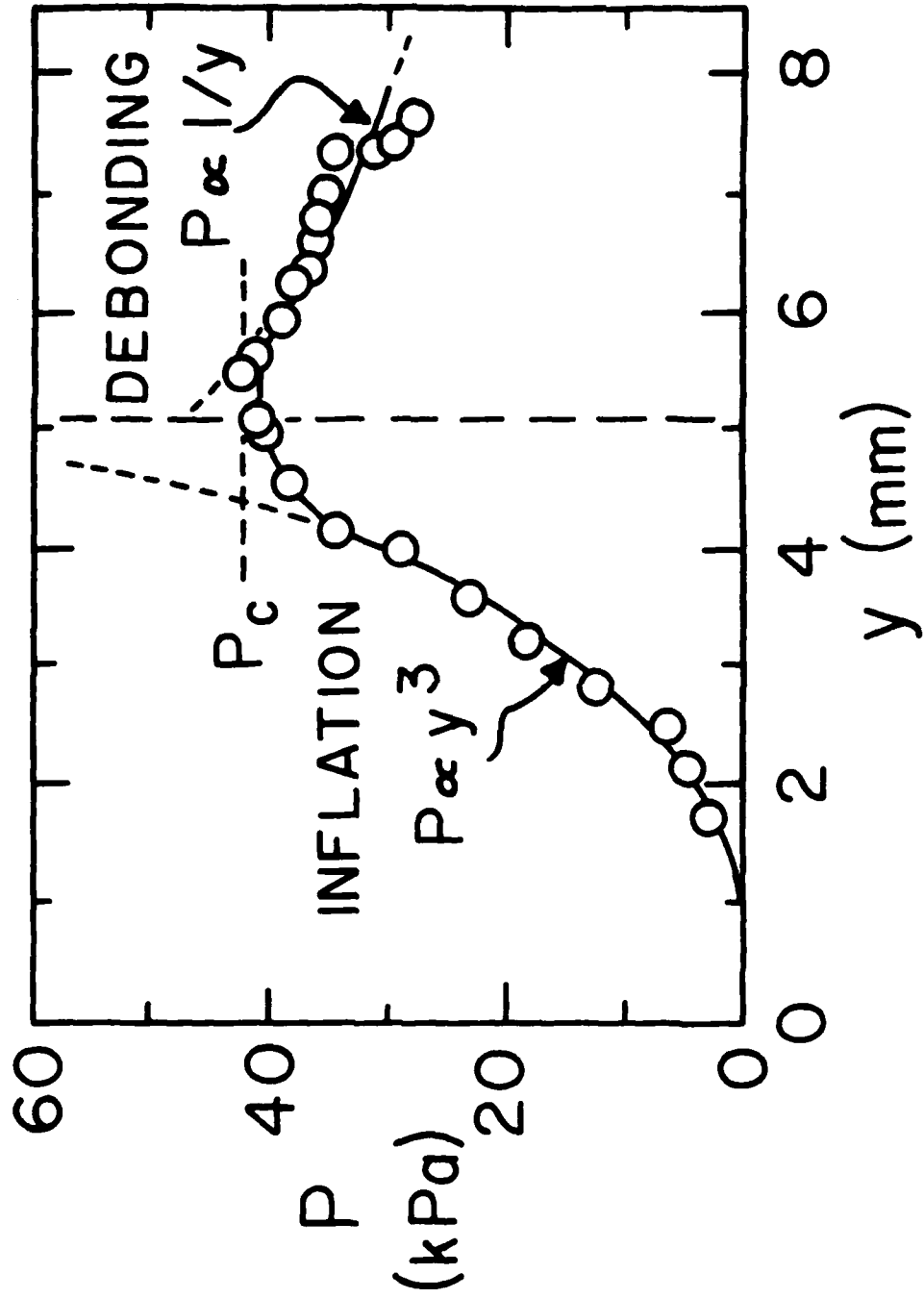


Figure 5

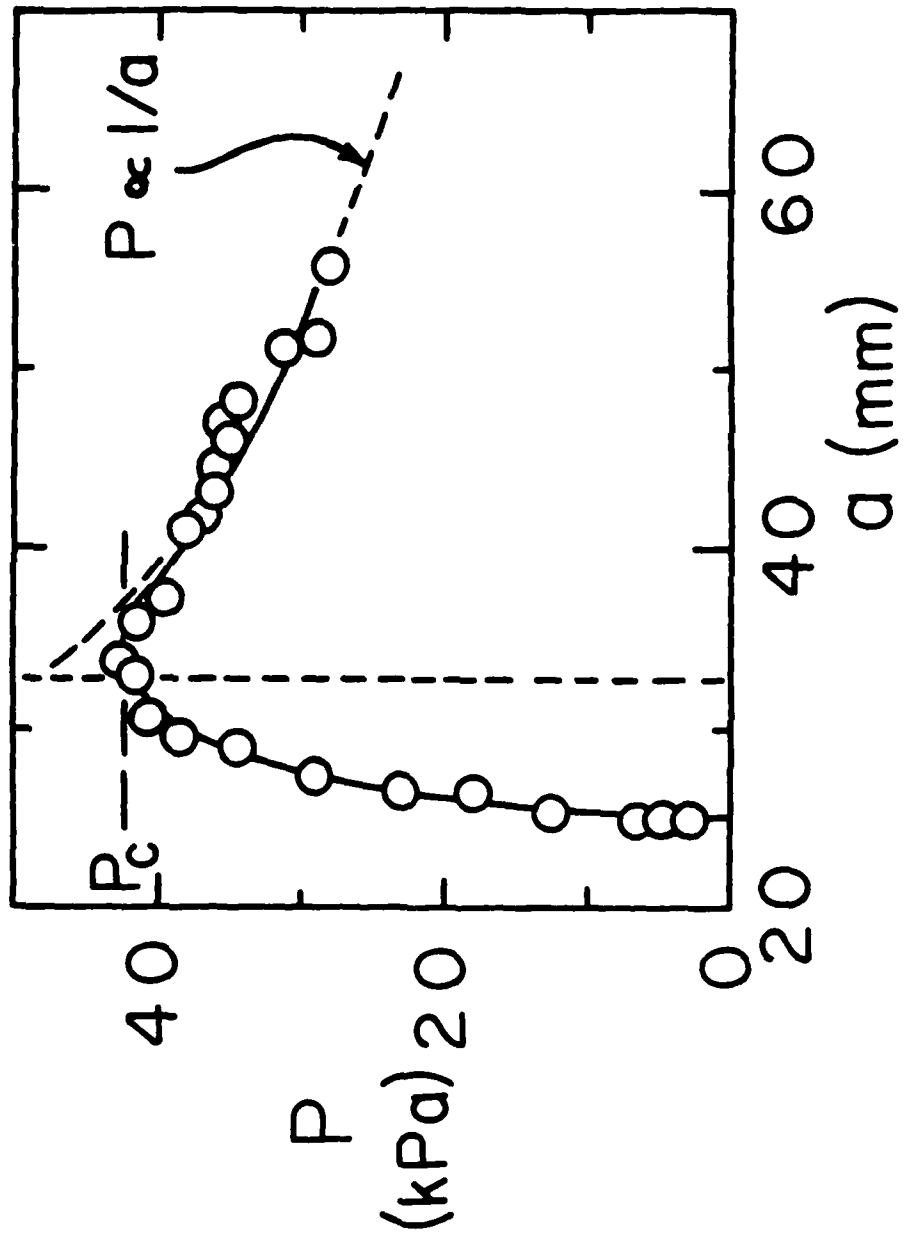


Figure 6

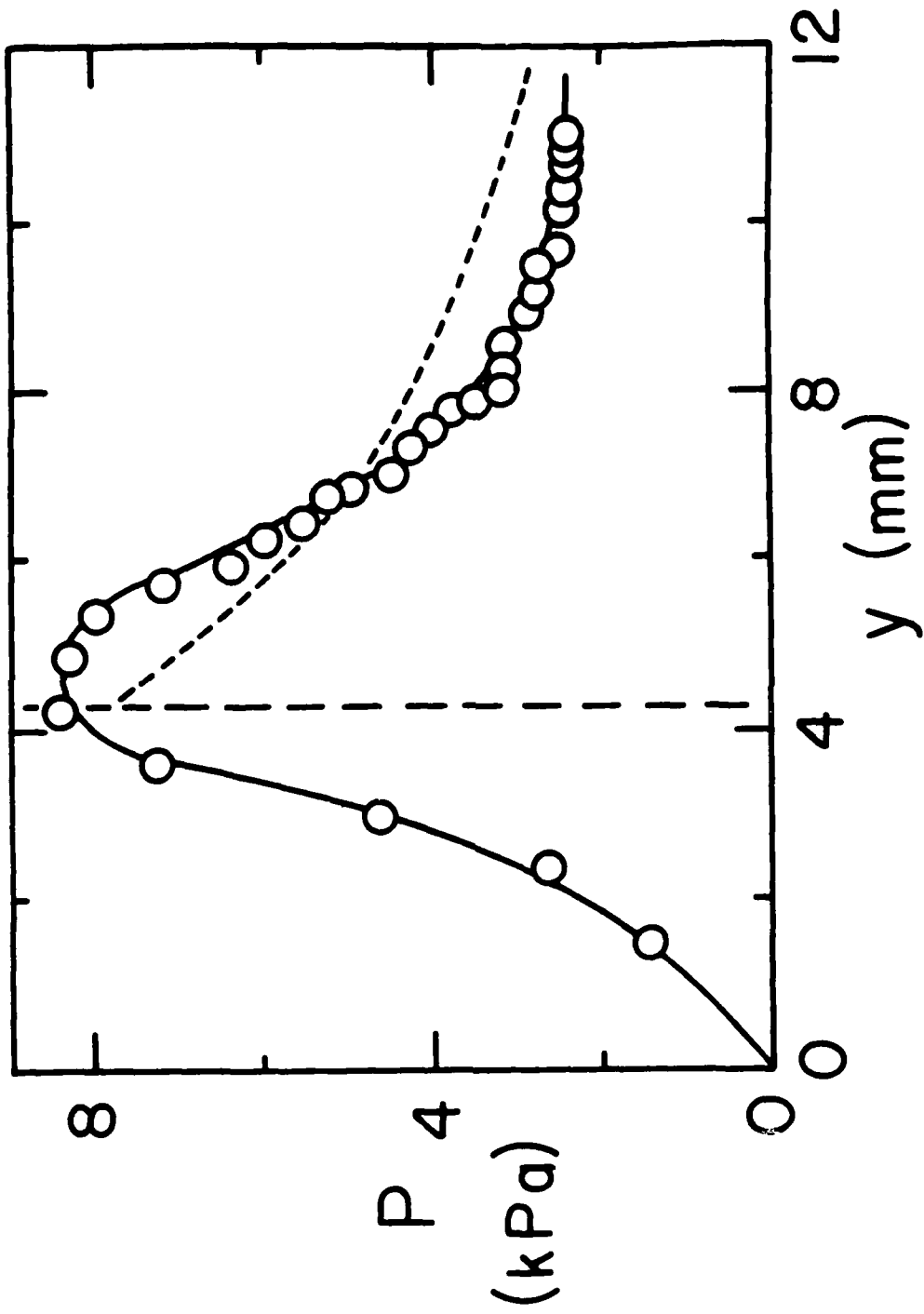


Figure 7

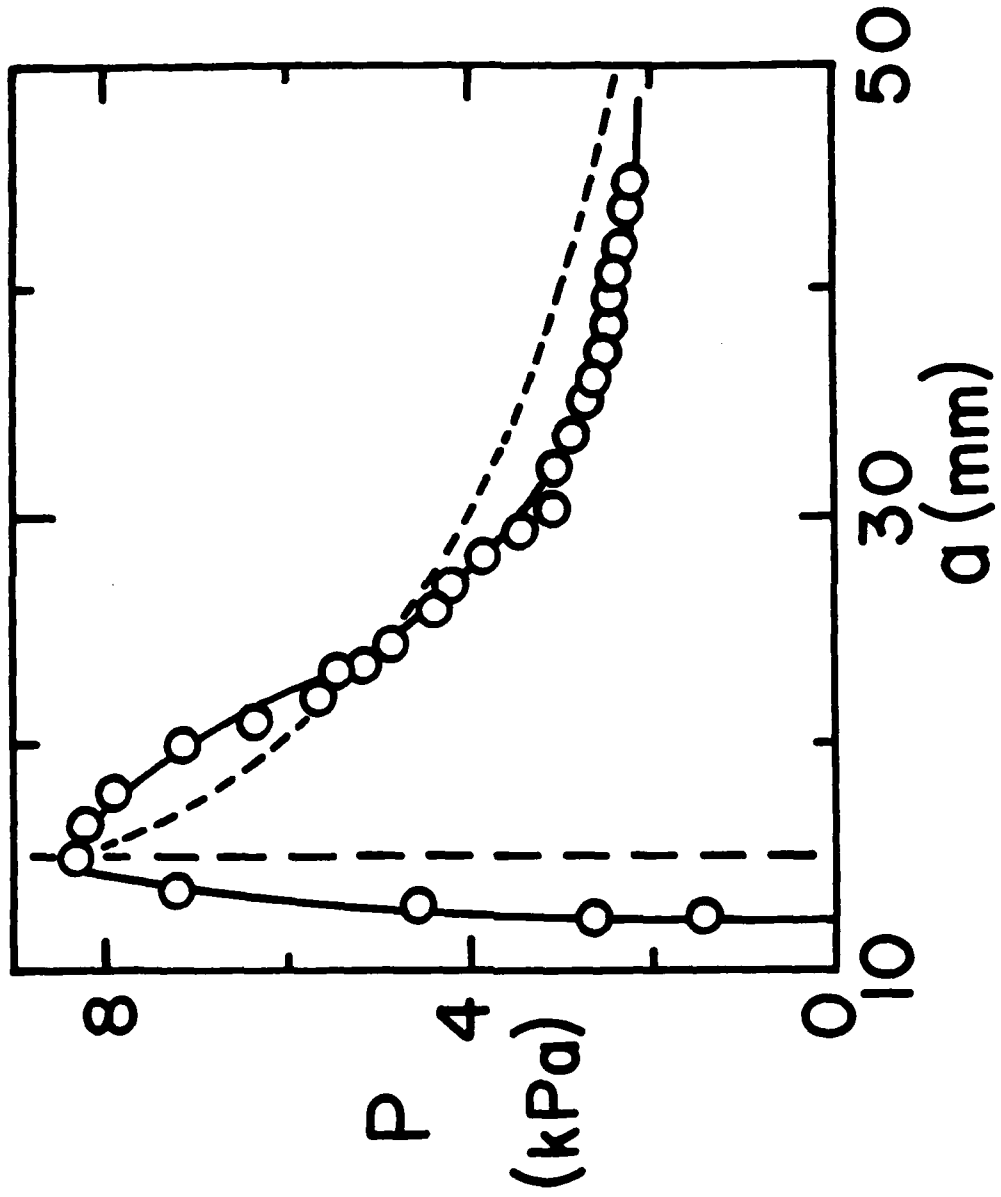


Figure 8



(DYN)

DISTRIBUTION LIST

Dr. R.S. Miller  
Office of Naval Research  
Code 432P  
Arlington, VA 22217  
(10 copies)

Dr. J. Pastine  
Naval Sea Systems Command  
Code 06R  
Washington, DC 20362

Dr. Kenneth D. Hartman  
Hercules Aerospace Division  
Hercules Incorporated  
Alleghany Ballistic Lab  
P.O. Box 210  
Washington, DC 21502

Mr. Otto K. Heiney  
AFATL-DLJG  
Elgin AFB, FL 32542

Dr. Merrill K. King  
Atlantic Research Corp.  
5390 Cherokee Avenue  
Alexandria, VA 22312

Dr. R.L. Lou  
Aerojet Strategic Propulsion Co.  
Bldg. 05025 - Dept 5400 - MS 167  
P.O. Box 15699C  
Sacramento, CA 95813

Dr. R. Olsen  
Aerojet Strategic Propulsion Co.  
Bldg. 05025 - Dept 5400 - MS 167  
P.O. Box 15699C  
Sacramento, CA 95813

Dr. Randy Peters  
Aerojet Strategic Propulsion Co.  
Bldg. 05025 - Dept 5400 - MS 167  
P.O. Box 15699C  
Sacramento, CA 95813

Dr. D. Mann  
U.S. Army Research Office  
Engineering Division  
Box 12211  
Research Triangle Park, NC 27709-2211

Dr. L.V. Schmidt  
Office of Naval Technology  
Code 07CT  
Arlington, VA 22217

JHU Applied Physics Laboratory  
ATTN: CPIA (Mr. T.W. Christian)  
Johns Hopkins Rd.  
Laurel, MD 20707

Dr. R. McGuire  
Lawrence Livermore Laboratory  
University of California  
Code L-324  
Livermore, CA 94550

P.A. Miller  
736 Leavenworth Street, #6  
San Francisco, CA 94109

Dr. W. Moniz  
Naval Research Lab.  
Code 6120  
Washington, DC 20375

Dr. K.F. Mueller  
Naval Surface Weapons Center  
Code R11  
White Oak  
Silver Spring, MD 20910

Prof. M. Nicol  
Dept. of Chemistry & Biochemistry  
University of California  
Los Angeles, CA 90024

Mr. L. Roslund  
Naval Surface Weapons Center  
Code R10C  
White Oak, Silver Spring, MD 20910

Dr. David C. Sayles  
Ballistic Missile Defense  
Advanced Technology Center  
P.O. Box 1500  
Huntsville, AL 35807

(DYN)

DISTRIBUTION LIST

Mr. R. Geisler  
ATTN: DY/MS-24  
AFRPL  
Edwards AFB, CA 93523

Naval Air Systems Command  
ATTN: Mr. Bertram P. Sobers  
NAVAIR-320G  
Jefferson Plaza 1, RM 472  
Washington, DC 20361

R.B. Steele  
Aerojet Strategic Propulsion Co.  
P.O. Box 15699C  
Sacramento, CA 95813

Mr. M. Stosz  
Naval Surface Weapons Center  
Code R10B  
White Oak  
Silver Spring, MD 20910

Mr. E.S. Sutton  
Thiokol Corporation  
Elkton Division  
P.O. Box 241  
Elkton, MD 21921

Dr. Grant Thompson  
Morton Thiokol, Inc.  
Wasatch Division  
MS 240 P.O. Box 524  
Brigham City, UT 84302

Dr. R.S. Valentini  
United Technologies Chemical Systems  
P.O. Box 50015  
San Jose, CA 95150-0015

Dr. R.F. Walker  
Chief, Energetic Materials Division  
DRSMC-LCE (D), B-3022  
USA ARDC  
Dover, NJ 07801

Dr. Janet Wall  
Code 012  
Director, Research Administration  
Naval Postgraduate School  
Monterey, CA 93943

Director  
US Army Ballistic Research Lab.  
ATTN: DRXBR-IBD  
Aberdeen Proving Ground, MD 21005

Commander  
US Army Missile Command  
ATTN: DRSMI-RKL  
Walter W. Wharton  
Redstone Arsenal, AL 35898

Dr. Ingo W. May  
Army Ballistic Research Lab.  
ARRADCOM  
Code DRXBR - 1BD  
Aberdeen Proving Ground, MD 21005

Dr. E. Zimet  
Office of Naval Technology  
Code 071  
Arlington, VA 22217

Dr. Ronald L. Derr  
Naval Weapons Center  
Code 389  
China Lake, CA 93555

T. Boggs  
Naval Weapons Center  
Code 389  
China Lake, CA 93555

Lee C. Estabrook, P.E.  
Morton Thiokol, Inc.  
P.O. Box 30058  
Shreveport, Louisiana 71130

Dr. J.R. West  
Morton Thiokol, Inc.  
P.O. Box 30058  
Shreveport, Louisiana 71130

Dr. D.D. Dillehay  
Morton Thiokol, Inc.  
Longhorn Division  
Marshall, TX 75670

G.T. Bowman  
Atlantic Research Corp.  
7511 Wellington Road  
Gainesville, VA 22065

(DYN)

DISTRIBUTION LIST

R.E. Shenton  
Atlantic Research Corp.  
7511 Wellington Road  
Gainesville, VA 22065

Mike Barnes  
Atlantic Research Corp.  
7511 Wellington Road  
Gainesville, VA 22065

Dr. Lionel Dickinson  
Naval Explosive Ordnance  
Disposal Tech. Center  
Code D  
Indian Head, MD 20340

Prof. J.T. Dickinson  
Washington State University  
Dept. of Physics 4  
Pullman, WA 99164-2814

M.H. Miles  
Dept. of Physics  
Washington State University  
Pullman, WA 99164-2814

Dr. T.F. Davidson  
Vice President, Technical  
Morton Thiokol, Inc.  
Aerospace Group  
110 North Wacker Drive  
Chicago, Illinois 60606

Mr. J. Consaga  
Naval Surface Weapons Center  
Code R-16  
Indian Head, MD 20640

Naval Sea Systems Command  
ATTN: Mr. Charles M. Christensen  
NAVSEA-62R2  
Crystal Plaza, Bldg. 6, Rm 806  
Washington, DC 20362

Mr. R. Beauregard  
Naval Sea Systems Command  
SEA 64E  
Washington, DC 20362

Brian Wheatley  
Atlantic Research Corp.  
7511 Wellington Road  
Gainesville, VA 22065

Mr. G. Edwards  
Naval Sea Systems Command  
Code 62R32  
Washington, DC 20362

C. Dickinson  
Naval Surface Weapons Center  
White Oak, Code R-13  
Silver Spring, MD 20910

Prof. John Deutch  
MIT  
Department of Chemistry  
Cambridge, MA 02139

Dr. E.H. deButts  
Hercules Aerospace Co.  
P.O. Box 27408  
Salt Lake City, UT 84127

David A. Flanigan  
Director, Advanced Technology  
Morton Thiokol, Inc.  
Aerospace Group  
110 North Wacker Drive  
Chicago, Illinois 60606

Dr. L.H. Caveny  
Air Force Office of Scientific  
Research  
Directorate of Aerospace Sciences  
Bolling Air Force Base  
Washington, DC 20332

W.G. Roger  
Code 5253  
Naval Ordnance Station  
Indian Head, MD 20640

Dr. Donald L. Ball  
Air Force Office of Scientific  
Research  
Directorate of Chemical &  
Atmospheric Sciences  
Bolling Air Force Base  
Washington, DC 20332

(DYN)

DISTRIBUTION LIST

Dr. Anthony J. Matuszko  
Air Force Office of Scientific Research  
Directorate of Chemical & Atmospheric  
Sciences  
Bolling Air Force Base  
Washington, DC 20332

Dr. Michael Chaykovsky  
Naval Surface Weapons Center  
Code R11  
White Oak  
Silver Spring, MD 20910

J.J. Rocchio  
USA Ballistic Research Lab.  
Aberdeen Proving Ground, MD 21005-5066

G.A. Zimmerman  
Aerojet Tactical Systems  
P.O. Box 13400  
Sacramento, CA 95813

B. Swanson  
INC-4 MS C-346  
Los Alamos National Laboratory  
Los Alamos, New Mexico 87545

Dr. James T. Bryant  
Naval Weapons Center  
Code 3205B  
China Lake, CA 93555

Dr. L. Rothstein  
Assistant Director  
Naval Explosives Dev. Engineering Dept.  
Naval Weapons Station  
Yorktown, VA 23691

Dr. M.J. Kamlet  
Naval Surface Weapons Center  
Code R11  
White Oak, Silver Spring, MD 20910

Dr. Henry Webster, III  
Manager, Chemical Sciences Branch  
ATTN: Code 5063  
Crane, IN 47522

Dr. A.L. Slafkosky  
Scientific Advisor  
Commandant of the Marine Corps  
Code RD-1  
Washington, DC 20380

Dr. H.G. Adolph  
Naval Surface Weapons Center  
Code R11  
White Oak  
Silver Spring, MD 20910

U.S. Army Research Office  
Chemical & Biological Sciences  
Division  
P.O. Box 12211  
Research Triangle Park, NC 27709

G. Butcher  
Hercules, Inc.  
MS X2H  
P.O. Box 98  
Magna, Utah 84044

W. Waesche  
Atlantic Research Corp.  
7511 Wellington Road  
Gainesville, VA 22065

Dr. John S. Wilkes, Jr.  
FJSRL/NC  
USAF Academy, CO 80840

Dr. H. Rosenwasser  
AIR-320R  
Naval Air Systems Command  
Washington, DC 20361

Dr. Joyce J. Kaufman  
The Johns Hopkins University  
Department of Chemistry  
Baltimore, MD 21218

Dr. A. Nielsen  
Naval Weapons Center  
Code 385  
China Lake, CA 93555

(DYN)

DISTRIBUTION LIST

K.D. Pae  
High Pressure Materials Research Lab.  
Rutgers University  
P.O. Box 909  
Piscataway, NJ 08854

Dr. John K. Dienes  
T-3, B216  
Los Alamos National Lab.  
P.O. Box 1663  
Los Alamos, NM 87544

A.N. Gent  
Institute Polymer Science  
University of Akron  
Akron, OH 44325

Dr. D.A. Shockey  
SRI International  
333 Ravenswood Ave.  
Menlo Park, CA 94025

Dr. R.B. Kruse  
Morton Thiokol, Inc.  
Huntsville Division  
Huntsville, AL 35807-7501

G. Butcher  
Hercules, Inc.  
P.O. Box 98  
Magna, UT 84044

W. Waesche  
Atlantic Research Corp.  
7511 Wellington Road  
Gainesville, VA 22065

Dr. R. Bernecker  
Naval Surface Weapons Center  
Code R13  
White Oak  
Silver Spring, MD 20910

Prof. Edward Price  
Georgia Institute of Tech.  
School of Aerospace Engineering  
Atlanta, GA 30332

J.A. Birkett  
Naval Ordnance Station  
Code 5253K  
Indian Head, MD 20640

Prof. R.W. Armstrong  
University of Maryland  
Dept. of Mechanical Engineering  
College Park, MD 20742

Herb Richter  
Code 385  
Naval Weapons Center  
China Lake, CA 93555

J.T. Rosenberg  
SRI International  
333 Ravenswood Ave.  
Menlo Park, CA 94025

G.A. Zimmerman  
Aerojet Tactical Systems  
P.O. Box 13400  
Sacramento, CA 95813

Prof. Kenneth Kuo  
Pennsylvania State University  
Dept. of Mechanical Engineering  
University Park, PA 16802

T.L. Boggs  
Naval Weapons Center  
Code 3891  
China Lake, CA 93555

(DYN)

DISTRIBUTION LIST

Dr. C.S. Coffey  
Naval Surface Weapons Center  
Code R13  
White Oak  
Silver Spring, MD 20910

D. Curran  
SRI International  
333 Ravenswood Avenue  
Menlo Park, CA 94025

E.L. Throckmorton  
Code SP-2731  
Strategic Systems Program Office  
Crystal Mall #3, RM 1048  
Washington, DC 23076

Dr. R. Martinson  
Lockheed Missiles and Space Co.  
Research and Development  
3251 Hanover Street  
Palo Alto, CA 94304

C. Gotzmer  
Naval Surface Weapons Center  
Code R-11  
White Oak  
Silver Spring, MD 20910

G.A. Lo  
3251 Hanover Street  
B204 Lockheed Palo Alto Research Lab  
Palo Alto, CA 94304

R.A. Schapery  
Civil Engineering Department  
Texas A&M University  
College Station, TX 77843

J.M. Culver  
Strategic Systems Projects Office  
SSPO/SP-2731  
Crystal Mall #3, RM 1048  
Washington, DC 20376

Prof. G.D. Duvall  
Washington State University  
Department of Physics  
Pullman, WA 99163

Dr. E. Martin  
Naval Weapons Center  
Code 3858  
China Lake, CA 93555

Dr. M. Farber  
135 W. Maple Avenue  
Monrovia, CA 91016

W.L. Elban  
Naval Surface Weapons Center  
White Oak, Bldg. 343  
Silver Spring, MD 20910

G.E. Manser  
Morton Thickett  
Wasatch Division  
P.O. Box 524  
Brigham City, UT 84302

R.G. Rosemeier  
Brimrose Corporation  
7720 Belair Road  
Baltimore, MD 20742

Administrative Contracting  
Officer (see contract for  
address)  
(1 copy)

Director  
Naval Research Laboratory  
Attn: Code 2627  
Washington, DC 20375  
(6 copies)

Defense Technical Information Center  
Bldg. 5, Cameron Station  
Alexandria, VA 22314  
(12 copies)

Dr. Robert Polvani  
National Bureau of Standards  
Metallurgy Division  
Washington, D.C. 20234

Dr. Y. Gupta  
Washington State University  
Department of Physics  
Pullman, WA 99163

END

12-86

DTIC